
Diffusion at the pore and at the pore-network scale

Jonas Schmid supervised by Alexander Schlaich

Institute for Computational Physics, University of Stuttgart

June 8, 2021

1 INTRODUCTION

The phenomenon of Brownian motion was described the first time in 1827 by Robert Brown, while observing pollen under a microscope[16]. Albert Einstein[4] and Marian Smoluchowski [13] came up first with a theoretical concept to describe Robert Browns observations, and connect them to a diffusion coefficient. In general, analytical solutions of Fick's laws of diffusion, only exist for restricted systems and not for diffusion through porous media. An illustration of gas diffusion through a single pore is given by Figure 1. Even in a single pore like in Figure 1, diffusion properties mostly can not be derived analytically due to interactions with the pore walls. Consequently, the description of diffusion in complex porous networks becomes difficult. Fundamental concepts of statistical physics like the time evolution given by the Fokker-Planck equation or the stochastic trajectory described by the Langevin equation become very challenging to solve in porous networks.

Complex systems with locally varying diffusion properties are generally not analytically solvable. To describe the diffusion in such systems, it is either necessary to approximate the system by an analytically solvable shape or to analyze the particular system with a computer simulation. For computer simulations, either MD simulations or random walk approaches can be used.

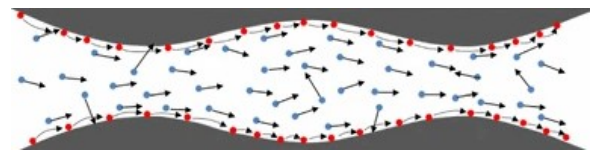


Figure 1: Gas diffusion through a pore, containing molecular interaction and interaction with the pore wall. [17]

In the first part, we will discuss different diffusion mechanisms, taking place in porous media, in the order of pore size. In the second part, diffusion properties for porous networks will be derived. Especially hierarchical porosity will be taken into account.

2 Diffusion Mechanisms in porous Media

An overview of diffusion mechanisms describing gas diffusion in a pore is given in Figure 2. Depending on the interaction strength of the gas with the pore and the relation between the pore diameter d and the free path length in the gas, different mechanisms can be derived. These diffusion mechanisms can be applied in filtering or separating different components of mixtures.

For pores smaller than the diameter of the gas molecules, molecular sieving is obtained (Figure 2, b). For a strong adsorption at the surface, sur-

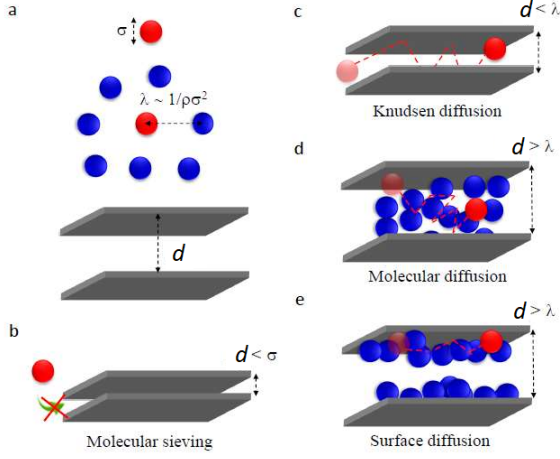


Figure 2: Different diffusion mechanisms describing gas diffusion through a pore. Depending on pore diameter and interaction with the wall, different diffusion mechanisms can be derived. [1]

face diffusion can be observed (Figure 2, e). The other gas diffusion mechanisms will be treated more in detail in the following.

2.1 Knudsen Diffusion and Slip Corrections

Knudsen diffusion is a diffusion mechanism describing the diffusion of a gas through a pore assuming a small pore radius. The diffusivity in this case can be derived from the diffusivity of a free gas. For a gas, the diffusion coefficient

$$D = \frac{\lambda \bar{v}}{3} = \frac{\lambda}{3} \sqrt{\frac{8k_B T}{\pi m}} \quad (1)$$

results from the kinetic theory of gases [8]. The mean free path $\lambda = 1/\sqrt{2}\rho\pi\sigma^2$ depends on the particle density ρ and the diameter σ of the particles. The average molecular speed \bar{v} is given by the Maxwell-Boltzmann distribution.

For a gas in a pore with a pore diameter $d < \lambda$, shown in Figure 2c the collisions with the pore wall are more frequent than collisions with other particles. The diffusion in such a pore is called Knudsen diffusion [9]. The diffusion coefficient for Knudsen diffusion in a cylindrical pore with the diameter d is given by

$$D_K = \frac{d}{3} \sqrt{\frac{8k_B T}{\pi m}}. \quad (2)$$

This diffusion coefficient can be extended for Knudsen flow in porous media with the pore radius D_P by introducing the material properties

tortuosity and porosity. The tortuosity τ describes the ratio between the length of the path through a porous medium and the direct line, connecting the start- and endpoint of the curve [3]. The porosity Φ describes the ratio between the volume of void-space and the total volume of the medium. The diffusivity D_{eff} of the porous medium is given by [3]

$$D_{\text{eff}} = \frac{\Phi}{\tau} D_K. \quad (3)$$

For derivation of the diffusion coefficient for Knudsen diffusion, we have assumed, that the particles are diffusely reflected at the pore surfaces. Only a fraction f of the colliding molecules is diffusely reflected, while the rest of the molecules are specularly reflected. This leads to a diffusion coefficient

$$D_{\text{eff}} = \frac{D_P}{3} \frac{\Phi}{\tau} \frac{2-f}{f} \sqrt{\frac{8k_B T}{\pi m}}, \quad (4)$$

where f is called tangential momentum accommodation factor. This factor depends on the potential of the pore surface and the gas molecules, but is mostly independent of the drift velocity of the gas molecules [14].

2.2 Combination of Knudsen diffusion and molecular diffusion

In larger pores ($d > \lambda$) like in Figure 2d, the diffusion consists of molecular diffusion described by the diffusion coefficient D_M as well as of Knudsen diffusion. The molecular diffusion can be described by viscous flow using the Stokes-Einstein equation with the temperature dependence $D_M \propto T$ [9]. Another form of molecular diffusion is activated diffusion. A particle is hopping on a lattice and needs to overcome a potential energy barrier E_a to move forward to the next position on the lattice. An exemplary one-dimensional energy landscape is shown in Figure 3. The temperature dependence of the diffusion coefficient $D_M \propto \exp[E_a/(k_B T)]$ is given by the Arrhenius law. [11] The diffusion coefficient D_c for such a combined regime is given by [9]

$$\frac{1}{D_c} \propto \frac{1}{D_K} + \frac{1}{D_M}. \quad (5)$$

While the temperature dependence of the Knudsen diffusion is given by $D_K \propto \sqrt{T}$.

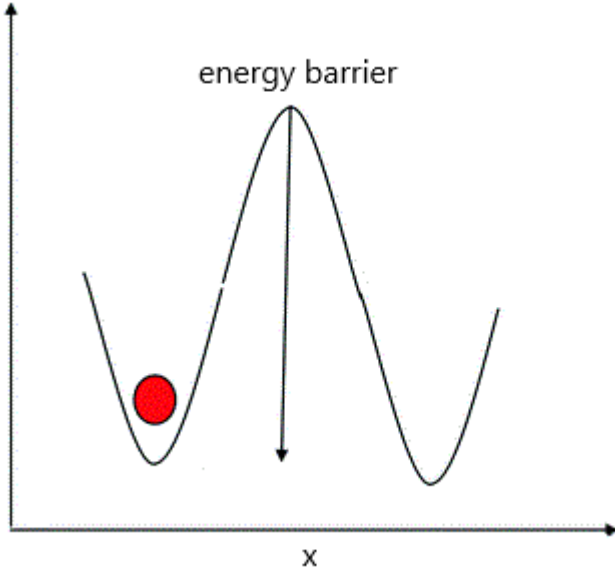


Figure 3: An example for the potential energy landscape of a lattice hopping system. The particle in the potential energy landscape needs to overcome the energy barrier to leave its initial place.[11]

2.3 Hydrodynamic Origin of Diffusion in Nanopores

Simulations of gas molecules in nanopores show that molecules do not behave like gas molecules, which collide with the interface and get reflected, as we assumed deriving the diffusion coefficient for the Knudsen dynamics. This is shown by molecular dynamics (MD) simulations of Lennard-Jones Methane in a cylindrical silica pore.[2] The density profile shows, that most of the methane molecules are localized at the potential minimum close to the silica surface.

Furthermore, different diffusivities in the previously described pore can be derived. By using equilibrium molecular dynamics (EMD) a transport coefficient can be obtained from the fluctuation axial streaming velocity via the Green-Kubo relation. This transport coefficient matches with the transport coefficient, which is obtained from a system with a constant axial acceleration by measuring the axial flux and the density of methane in the pore. The results also matches with the transport properties measured in a finite capillary connected to a dual control. In this case, two control volumes on the opposite sides of the pore with different particle densities cause a flux through the pore. We also expect the same diffusivity for all three methods from statistical physics.

For the total diffusion coefficient, an expression containing viscous flow as well as slip flow can be written as[2]

$$D_{\text{tot}}(\hat{\rho}) = \frac{2k_B T}{R_s^2 \hat{\rho}} \left[\frac{1}{k \rho_0 r_0} \left(\int_0^{r_0} r \rho(r) dr \right)^2 + \int_0^{r_0} \frac{dr}{r \eta(r)} \left(\int_0^r r' \rho(r') dr' \right)^2 \right]. \quad (6)$$

The part of the diffusion coefficient (6), which is received by assuming viscous flow only matches with the value of the simulation for high densities of methane (lower part of (6)). This term vanishes for small densities, while the simulations show a non-vanishing behavior for small densities caused by slip-effects. The degree of slip is considered in the upper part of the term for the diffusion coefficient (6).

To calculate the diffusivity given in (6), it is necessary to know the radial density profile $\rho(r)$ as well as the radial viscosity $\eta(r)$.

For small densities if we replace $\rho(r) \propto e^{\frac{a\Phi_m}{k_B T}}$ by the Boltzmann distribution, we receive a diffusivity

$$D \propto e^{a\Phi_m/(k_B T)} \quad (7)$$

with an $0 < a < 1$ and the energy Φ_m at the potential minimum. We obtain activated diffusion with the effective activation energy/energy barrier of $E_D = a|\Phi_m|$.

2.4 Motion through diffusive landscapes

Movement in porous media mostly is subject to a diffusive landscape and not a constant diffusivity. The diffusion coefficient $D(\mathbf{r}, t)$ in porous media can be depending on place as well as time. Thus, a particle trajectory runs through different areas with different diffusivities, illustrated on the left side in Figure 4.

A measurable property is the self-correlation function given by

$$G(\mathbf{r}, t) = \langle \delta(\mathbf{R}(t) - \mathbf{R}(0) - \mathbf{r}) \rangle. \quad (8)$$

This characteristic can be obtained from computer simulations or in an experimental way using confocal microscopy, which tracks particles in real space and time. The temporal development

of $G(\mathbf{r}, t)$ can also be described by the Fokker-Planck equation. Unfortunately, no common solution for this equation exists.

An experimentally more significant property is given by the Fourier transformation of $G(\mathbf{r}, t)$, which reads

$$I(\mathbf{q}, t) = \int G(\mathbf{r}, t) e^{i\mathbf{q}\mathbf{r}} d\mathbf{r}. \quad (9)$$

This intermediate scattering function can be obtained using pulsed-field gradient nuclear magnetic resonance (PFG NMR) measurements.

Due to the absence of a general analytical solution, just approximated systems can be treated analytically. The diffusive landscape can often be divided in domains (Figure 4, left). Where the potential energy and the diffusivity is set to a constant average value. In the following, domains with similar properties are clustered into a finite number of diffusive states [12]. The transition between the states is characterized by the mean first-passage time. This time describes the mean time the system remains in a certain state before leaving it. A connected network of states (Figure 4, right) arises. Especially the limiting cases of very fast and very slow switching between states compared to the intra-domain dynamics can be studied [12]. The slow switching limit is defined for systems, in which for all states i the mean first-passage time t_{FP}^i is much larger than the intra-domain relaxation time $t_{\text{rel}}^i \propto 1/D_i q^2$. In other words, the system relaxes to equilibrium in each state before switching into another state. The intermediate scattering function is given by

$$I_{\text{slow}}(\mathbf{q}, t) = \sum_{i=0}^M c_i e^{-D_i q^2 t}. \quad (10)$$

Where c_i is the equilibrium fraction of particles in domain i .

The fast switching limit applies to systems with $t_{\text{FP}}^i \ll t_{\text{rel}}^i$ for all domains. In this case, the trajectory averages over all domains respectively all states mostly instantaneously. The intermediate scattering function is given by

$$I_{\text{fast}}(\mathbf{q}, t) = e^{-\sum_{i=0}^M c_i D_i q^2 t} = e^{-\bar{D} q^2 t}. \quad (11)$$

We obtain an effective medium described by the average diffusivity $\bar{D} = \sum_{i=0}^M c_i D_i$. Systems, which combine surface diffusion and diffusion in the free pore space, assuming the displacements in both regimes are uncorrelated, lead to the same relation for the average diffusivity.

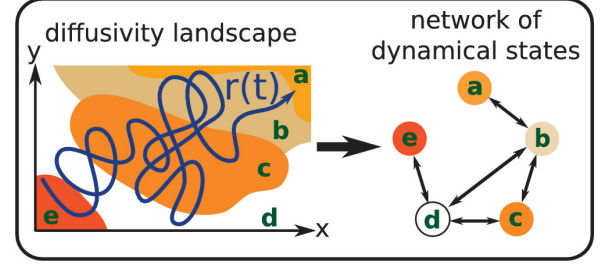


Figure 4: The left side shows a trajectory through a diffusive landscape divided into the domains $a - e$. The right picture shows the network of dynamical states obtained from the landscape on the left. [12]

2.5 Molecular intermittent dynamics of water

The interaction of confined water with a strongly adsorbing surface is present in many applications like nanofiltration or phase separation. Many properties of confined water, like in a nanopore, can be expressed a proportion of adsorbed water close to the surface with a reduced mobility and a proportion of water in the confined bulk. The time evolution can be described by the indicator function $I(t)$. Where $I(t)$ equals one for equals one in the adsorbed state and zero in the bulk state. An example for the behavior of the indicator function is given in Figure 5. The auto-correlation function

$$C(t) = \overline{I(t)I(0)} / \eta_A \quad (12)$$

with $\eta_A = \frac{\tau_A}{\tau_A + \tau_B}$ characterizes the statistical behavior of the dynamics. The values τ_A and τ_B are the average time spent either in the bulk or in the adsorbed phase before leaving the respectively state. By describing the adsorption of a molecule from the bulk, a known approximation for an infinite flat surface is used. Further, it is assumed, that the adsorption and the relocation of molecules is statistically independent. This leads us to the Fourier transformation of $C(t)$ given by

$$\begin{aligned} \mathcal{F}(C)(\omega) &= J(\omega) \\ &= \frac{2\tau_A^2 D / \delta^2}{(\omega/\omega_0)^{1/2} + (\omega/\omega_0) + 1/2(\omega/\omega_0)(3/2)}. \end{aligned} \quad (13)$$

The diffusivity in the confined bulk is given D and the starting distance to the surface of a particle is given by δ . The characteristic frequency is given by $\omega_0 = \delta^2 / (2D\tau_A^2)$. Additionally the function $J(\omega)$ can be obtained via PFG NMR measurements.

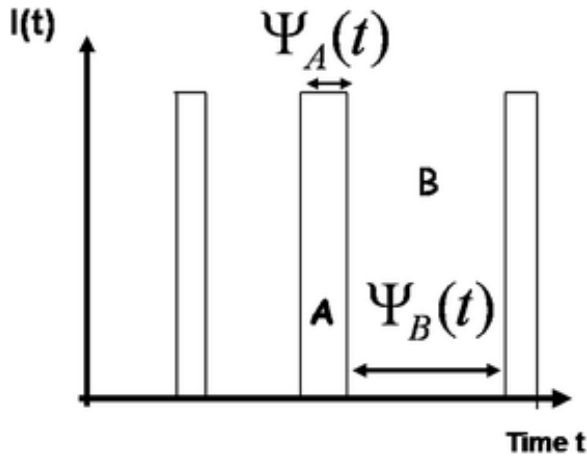


Figure 5: Indicator function $I(t)$, which describes whether an atom is adsorbed at the surface (state A) or unbound in the bulk (state B). The probability distribution functions $\Psi_A(t)$ and $\Psi_B(t)$ characterize the adsorption and bulk relocation. [7]

The computation of $J(\omega)$ from direct correlations for the simulated system shows, that the theoretical expression (13) holds, if the first two layers of water are defined as the adsorbed domain. This approach defines an independent adsorption region in exchange with the bulk flow in a confined liquid. Furthermore, properties like τ_A , which quantify the interaction between adsorbed phase and confined bulk, can be obtained. Furthermore, the statistical behavior for long times can be expressed by the analytical solution, while simulations for long times are very expensive due to computational resources.

2.6 Free Volume Theory

Another behavior of diffusion can be studied in ultra-confining media with strong adsorption. An example for such a kind of diffusion are alkane mixtures in a model of kerogen [10], visualized in Figure 6. The theory of recovering hydrocarbons from such an ultra-confining and disordered porosity like in shale gas is the basis of hydraulic fracturing.

In such an ultra-confining media, cross-correlations between different adsorbed molecules are negligible due to the strong interaction with the medium. As a consequence the collective diffusivity can be estimated from the self diffusion as $D_c \approx D_s$. The free volume

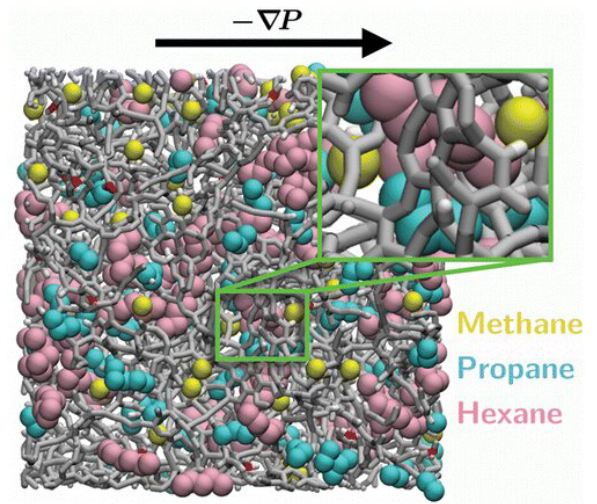


Figure 6: Mixture of methane, propane and hexane (yellow, blue and pink) confined in kerogen (gray red and white bounds) [10].

theory provides the expression

$$D_s = D_{s,0} e^{-\alpha \frac{NV_{\text{alk}}}{V_{\text{free}}}} \quad (14)$$

for a pure alkane of N molecules with the volume V_{alk} . The available volume V_{free} and the self-diffusivity $D_{s,0}$ of an isolated molecule contribute to the expression. The coefficient α quantifies the overlap between different molecules. This coefficient is only dependent of the fluid type and the surface of the medium. Consequently one factor α is sufficient to describe the multi-component case. For component i with the self-diffusivity $D_{s,0}^i$ of the mixture results the diffusion coefficient

$$D_s^i = D_{s,0}^i e^{-\alpha \frac{V_{\text{mix}}}{V_{\text{free}}}}, \quad (15)$$

where V_{mix} is the volume taken by the mixture. The agreement with simulations of confined alkanes is shown in Figure 7.

3 Diffusion on a pore Network Scale

3.1 Hierarchical Porosity

For the description of diffusion on a pore network scale, we will deal particularly with hierarchical structures. These structures consist of porous structures in different length scales. An example are hierarchical silica monoliths (Figure 8) [6]. Silica monoliths consist of an inter-skeleton macroscopic porous structure. Additionally the

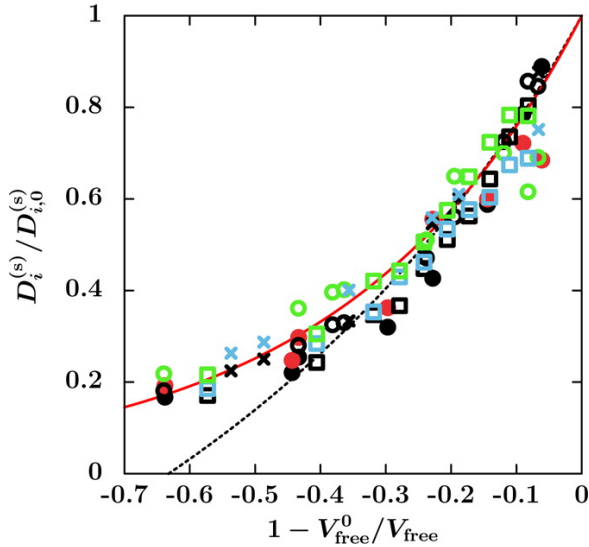


Figure 7: Self-diffusivity as a function of the free volume fraction for different mixtures of alkanes. The solid red line shows the free volume theory, while the black dashed line shows the result of a surface diffusion model. [10]

intra-skeleton structure shows to be mesoporous. In such a structure, one is mostly interested in the macroscopic properties, especially in the context of application of such media. It will be shown, that for the macroscopic diffusion, the dynamics in the mesopore space is not negligible.

First, we will have a look on experimental data of the diffusivity of cyclohexane in a hierarchical structure with pores in multiple length scales. In Figure 9 the effective diffusivity D_{eff} over a long range against the relative pressure. One line shows the properties while increasing the pressure in the system, while the other line shows the properties while decreasing the pressure in the system. The long range diffusivity depends on the relative number of molecules p_{inter} in the in the macroporous void space and the macroscopic diffusion coefficient D_{inter} is given by[6]

$$D_{\text{eff}} \approx p_{\text{inter}} D_{\text{inter}}. \quad (16)$$

In this case, the diffusivity in the mesopores is small compared to the diffusivity in the macroporous void space. The steep increase of the diffusivity, while decreasing the pressure from a relative pressure of $P/P_0 = 0.3$, can be associated with fluid pouring out of the mesopores. The connected increase of p_{inter} consequences an increase in the diffusivity. For a relative pressure relative pressure of $P/P_0 = 0.3$ the maximal filling in the mesopores is reached ($\Theta = 1$). Therefore the dif-

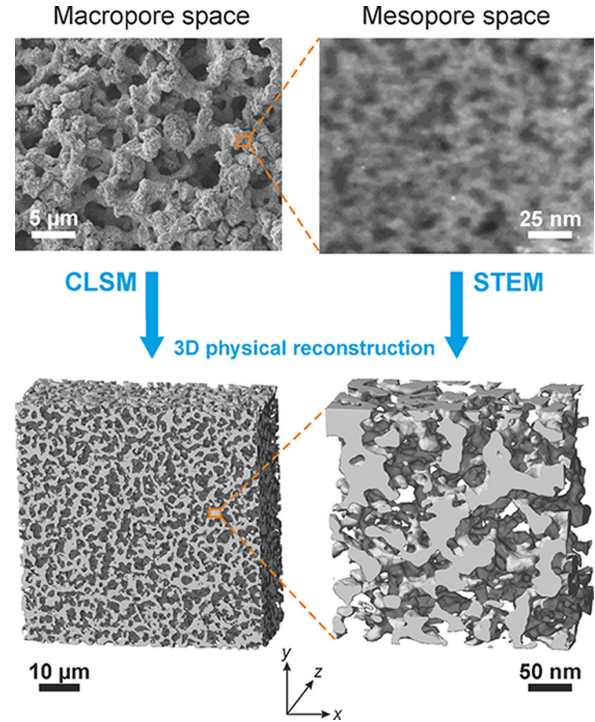


Figure 8: Physical reconstruction of hierarchical silica monoliths. Macropore space and mesopore space are illustrated separately in the specific length scale. [15]

fusivity stays constant with increasing pressure.

Investigations of special networks can also lead to differentiating diffusion properties. For example in continuous space of nanopores with larger pores embedded. In such a media, an increasing adsorption does not consequently lead to a decreasing diffusivity.

Also a diffusion hysteresis can be obtained in hierarchical materials. For special structures, the hysteresis is much more clear than for the system shown in Figure 9. Without discussing the explicit diffusion behavior for different geometries we will now study a numerical approach to describe the diffusion in hierarchical structures.

3.2 Random Walks

While dynamics in mesopores can be obtained by MD simulations, which compute the interaction between every molecule, involved in the system, such simulations are not suitable for large systems due to computational limitations. Consequently a simulation method is necessary, which does not require a recalculation interaction between every molecule in the system. A suitable method is generalizing the interaction with other particles by

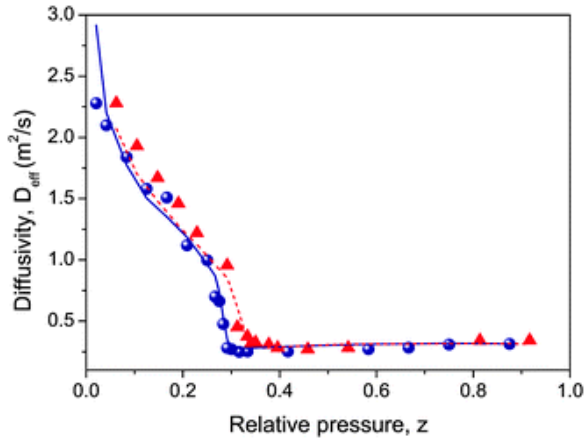


Figure 9: Effective diffusivity of cyclohexane in a hierarchical porous medium during adsorption (triangles) and desorption (circles). The relative pressure $z = P/P_0$ is defined using $P_0 = 6.6\text{kPa}$ [6].

random walk.

Random walk methods are based on the equivalence between the simulated trajectory and the description of the time evolution of the probability density function, given by the Fokker-Planck equation. The Fokker-Planck equation, which describes a particle position distribution $P(\mathbf{x}, t) = \langle \delta[\mathbf{x} - \mathbf{x}(t)] \rangle$ is called the Smoluchowski equation and reads[5]

$$\frac{\partial}{\partial t} P(\mathbf{x}, t) = [-\nabla \mathbf{A}(\mathbf{x}) + \nabla \otimes \nabla \mathbf{B}(\mathbf{x})] P(\mathbf{x}, t). \quad (17)$$

The components of a drift vector are denoted as $\mathbf{A}(\mathbf{x})$, while the components of the diffusion tensor are denoted by the components $\mathbf{B}(\mathbf{x})$. This equation holds for a negligible inertial force. For systems with a relevant inertial force, the diffusion of the system is described by the Kramers equation[5]. An analytic solution solution for the Fokker-Planck equation exists only in simplified cases like lower dimensional systems or locally independent drift and diffusion. It can be shown, that the Smoluchowski equation is equivalent to the Langevin equation

$$\frac{d\mathbf{x}(t)}{dt} = \mathbf{A}[\mathbf{x}(t)] + (2\mathbf{B}[\mathbf{x}(t)])^{1/2} \xi(t). \quad (18)$$

The Langevin equation gives an equation of motion for a single particle interacting randomly with the surrounding particles. In this equation of motion $\xi(t)$ describes a Gaussian white noise with the properties $\langle \xi(t) \rangle = \mathbf{0}$ and $\langle \xi_i(t) \xi_j(t') \rangle = \delta_{ij} \delta(t - t')$.

The interaction with other particles is generalized this term, including the Gaussian white noise. The Langevin equation (18) for a zero-drift system with constant diffusion coefficient D is given by

$$\frac{d\mathbf{x}(t)}{dt} = (2dD)^{1/2} \xi(t). \quad (19)$$

The mean square displacement of system described via (19) is given by the Einstein equation

$$\langle \mathbf{x}^2 \rangle = 2dDt. \quad (20)$$

The generalization of the interaction with other particles makes it possible to simulate dynamics even in large systems. It should be considered, that molecular effects like the interaction with a surface can be taken into account by the diffusion coefficient D . An example of using random walks in porous media will be given in the following chapter.

3.2.1 From Interfacial Dynamics to Hierarchical Porosity

In this approach, the results of MD simulation in molecular length space are implemented in random walk simulations in larger length scales to finally receive a macroscopic diffusion. The physical structure of the investigated porous media is shown in Figure 8.[15]

Detailed information about the interaction between the liquid and the interface are gained using MD simulation on an reserved-phase liquid chromatography (RPLC) model. These simulations are limited to a simple structure like a silt or a cylinder. The interface is given by a long alkyl chains bound on a silica surface. The liquid phase contains a mixture of water and organic molecules. These simulations yield to a diffusion coefficient parallel and a density to the surface (Figure 10), dependent on the distance to the interacting surface. In this case an area of ultra fast surface diffusion can be observed between the surface and the bulk region ($z > 2.5\text{ nm}$). In this region, the diffusion coefficient exceeds even the bulk diffusivity.

The effective diffusion coefficient in the mesopore space can be calculated by simulating a random walk. The diffusion coefficient, which is inserted in the equation of motion (19) is obtained by the previous MD simulation. To enable that, the mesopore space between the pore wall and the bulk region is split into different regions, dependent

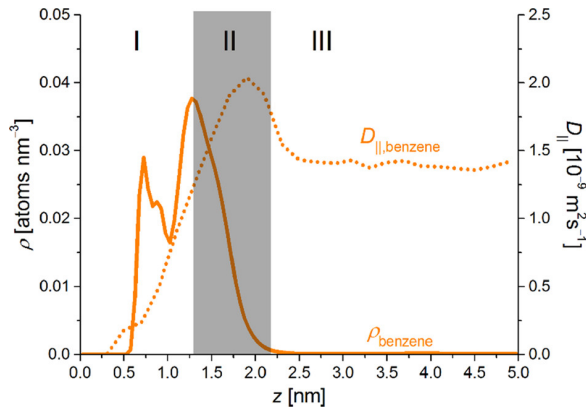


Figure 10: Surface-parallel diffusivity and number density of a benzene-water mixture in a slit-pore model. [15]

on their distance to the pore wall. In each voxel, the average value of the diffusivity and density is obtained from the MD simulation (Figure 10 and used for the random walk. The effective mesopore diffusivity D_{meso} is computed from the trajectories obtained by the random walk simulation. The calculation of the effective diffusion coefficient in the mesopores is done using the Einstein equation (20).

The effective macroscopic diffusion coefficient D_{bed} is received similar as D_{meso} . For the mesoporous space the diffusivity D_{meso} is obtained, while for the void macroscopic space, the bulk diffusivity D_{bulk} obtained from the MD simulations is assumed. The long time limit for the diffusivity is attained a lot earlier in this simulation than in the simulation of D_{meso} .

The result of such an approach is shown in Figure 11. The reference line D_{macro} represents the macroscopic diffusivity, assuming impermeable mesopore space using passive point-like tracers. It is shown, that the macroscopic diffusivity is increasing with the density of hydrocarbons in the mobile phases, which is causing an increase of the elution strength of the mobile phase. For a low elution, the effective diffusivity is less than the value D_{macro} . The reason is that many molecules are trapped in the mesopore with a low diffusivity. The diffusion through the mesopores causes a rise of the total diffusion only for a mobile phase with a high elution strength caused by ultra fast surface diffusion in mesopore space.

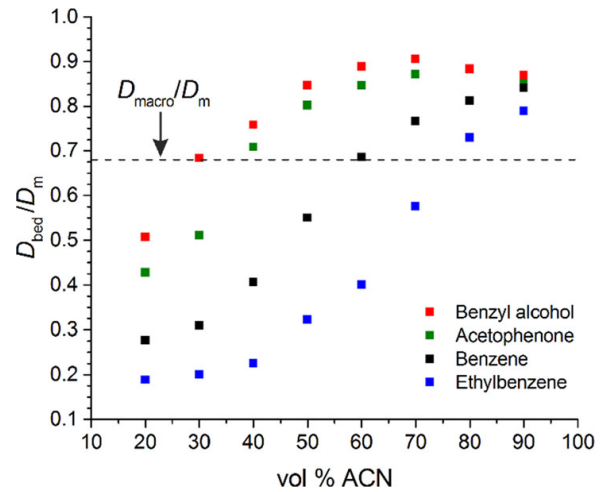


Figure 11: Effective macroscopic diffusivities for different mixtures of alkanes and water in the hierarchical porosity given by Figure 8. The dotted line marks the diffusivity assuming the mesopores as impermeable walls. [15]

4 Conclusion

In this handout, we have analyzed different diffusion behaviors on the single pore length scale. Like already mentioned in the beginning, complex systems like they occur in applied systems are mostly not analytically solvable in general. Dependent on the pore structure as well as interactions between the pore surface and the mobile phase, properties of diffusion distinguish fundamentally. Consequently there is no general way to describe diffusion in a mesopore length scale. On the mesopore scale at least MD simulations can be used to obtain a distribution for the diffusion in the system. The simulated data then, can be related to known concepts of diffusion.

In contrast to single pores, MD simulation are not applicable on macroscopic systems. In order to that numerical investigations on macroscopic systems require another method to describe the dynamics in the system. For example random walks can give an idea of the dynamics in macroscopic systems.

By studying hierarchical systems, it is obtained, that even for diffusion on a macroscopic scale, diffusion effects in mesopores and micropores are not negligible. This is an important point, especially if we look at applications of porous media for example in engineering.

Bibliography

- [1] Schlaich et al. 'in preparation'.
- [2] Suresh K. Bhatia and David Nicholson. "Hydrodynamic Origin of Diffusion in Nanopores". In: *Phys. Rev. Lett.* 90 (1 2003), p. 016105.
- [3] Roberto Cunningham. *Diffusion in Gases and Porous Media*. Springer US, 1980. DOI: 10.1007/978-1-4757-4983-0.
- [4] A. Einstein. "Über die von der molekularkinetischen Theorie der Wärme geforderte Bewegung von in ruhenden Flüssigkeiten suspendierten Teilchen". In: *Annalen der Physik* 322.8 (1905), pp. 549–560. DOI: <https://doi.org/10.1002/andp.19053220806>. eprint: <https://onlinelibrary.wiley.com/doi/pdf/10.1002/andp.19053220806>. URL: <https://onlinelibrary.wiley.com/doi/abs/10.1002/andp.19053220806>.
- [5] Risken H. *The Fokker-Planck Equation: Methods of Solution and Applications Second Edition*. Springer, 1989.
- [6] Jörg Kärger and Rustem Valiullin. "Mass transfer in mesoporous materials: the benefit of microscopic diffusion measurement". In: *Chem. Soc. Rev.* 42 (9 2013), pp. 4172–4197. DOI: 10.1039/C3CS35326E.
- [7] P. Levitz et al. "Molecular intermittent dynamics of interfacial water: probing adsorption and bulk confinement". In: *Soft Matter* 9 (36 2013), pp. 8654–8663. DOI: 10.1039/C3SM51940F.
- [8] R.L. Liboff. *Kinetic Theory: Classical, Quantum, and Relativistic Descriptions*. Springer-Verlag New York, 2003. DOI: 10.1007/b97467.
- [9] Endre Nagy. "Chapter 11 - Membrane Contactors". In: *Basic Equations of Mass Transport Through a Membrane Layer (Second Edition)*. Ed. by Endre Nagy. Second Edition. Elsevier, 2019. ISBN: 978-0-12-813722-2. DOI: <https://doi.org/10.1016/B978-0-12-813722-2.00011-X>. URL: <https://www.sciencedirect.com/science/article/pii/B978012813722200011X>.
- [10] Amaël Obliger et al. "Free Volume Theory of Hydrocarbon Mixture Transport in Nanoporous Materials". In: *The Journal of Physical Chemistry Letters* 7.19 (2016). PMID: 27570884, pp. 3712–3717. DOI: 10.1021/acs.jpcllett.6b01684.
- [11] Joshua Pelleg. *Mechanism of Diffusion*. Springer, Cham, 2015. DOI: https://doi.org/10.1007/978-3-319-18437-1_4.
- [12] Felix Roosen-Runge, Dominique J. Bicout, and Jean-Louis Barrat. "Analytical correlation functions for motion through diffusivity landscapes". In: *The Journal of Chemical Physics* 144.20 (2016), p. 204109. DOI: 10.1063/1.4950889. URL: <https://doi.org/10.1063/1.4950889>.
- [13] M. von Smoluchowski. "Zur kinetischen Theorie der Brownschen Molekularbewegung und der Suspensionen". In: *Annalen der Physik* 326.14 (1906), pp. 756–780. DOI: <https://doi.org/10.1002/andp.19063261405>. eprint: <https://onlinelibrary.wiley.com/doi/pdf/10.1002/andp.19063261405>. URL: <https://onlinelibrary.wiley.com/doi/abs/10.1002/andp.19063261405>.
- [14] Wojciech Sobieski. "The use of Path Tracking Method for determining the tortuosity field in a porous bed." in: *Granular Matter* 18 (July 2016). DOI: 10.1007/s10035-016-0668-3.
- [15] Ulrich Tallarek et al. "Multiscale Simulation of Diffusion in Porous Media: From Interfacial Dynamics to Hierarchical Porosity". In: *The Journal of Physical Chemistry C* 123.24 (2019), pp. 15099–15112. DOI: 10.1021/acs.jpcc.9b03250.
- [16] Robert Brown F.R.S. Hon. M.R.S.E. R.I. Acad. V.P.L.S. "XXVII. A brief account of microscopical observations made in the months of June, July and August 1827, on the particles contained in the pollen of plants; and on the general existence of active molecules in organic and inorganic bodies". In: *The Philosophical Magazine* 4.21 (1828), pp. 161–173. DOI: 10.1080/14786442808674769. URL: <https://doi.org/10.1080/14786442808674769>.

- [17] Yudong Yuan, Nima Gholizadeh Doonechaly, and Sheik Rahman. “An Analytical Model of Apparent Gas Permeability for Tight Porous Media”. In: *Transport in Porous Media* 111.1 (2016), pp. 193–214. DOI: 10.1007/s11242-015-0589-3. URL: <https://doi.org/10.1007/s11242-015-0589-3>.